MOLECULAR AND CELLULAR BIOLOGY, June 1990, p. 3194–3203
0270-7306/90/063194-10$02.00/0

Vol. 10, No. 6

Sequence and Functional Analysis of the Positively Acting Regulatory Gene *amdR* from *Aspergillus nidulans*

ALEX ANDRIANOPOULOS AND MICHAEL J. HYNES*

Department of Genetics, University of Melbourne, Parkville, Victoria 3052, Australia

Received 27 November 1989/Accepted 14 March 1990

The positively acting regulatory gene *amdR* of *Aspergillus nidulans* coordinately regulates the expression of five structural genes involved in the catabolism of certain amides (*amdS*), omega amino acids (*gatA* and *gabA*), and lactams (*lamA* and *lamB*) in the presence of omega amino acid inducers. Analysis of the *amdR* gene showed that it contains three small introns, heterogeneous 5′ and 3′ transcription sites, and multiple AUG codons prior to the major AUG initiator. The predicted *amdR* protein sequence has a cysteine-rich "zinc finger" DNA-binding motif at the amino-terminal end, four putative acidic transcription activation motifs in the carboxyl-terminal half, and two sequences homologous to the simian virus 40 large T antigen nuclear localization motif. These nuclear localization sequences overlap the cysteine-rich DNA-binding motif. A series of 5′, 3′, and internal deletions were examined in vivo for transcription activator function and showed that the *amdR* product contains at least two activation regions in the carboxyl-terminal half. Each of these activator regions may function independently, but both are required for wild-type levels of transcription activation. A number of the *amdR* deletion products were found to compete with the wild-type *amdR* product in vivo. Development of a rapid method for the localization of *amdR* mutations is presented, and using this technique, we localized and sequenced the mutation in the semiconstitutive *amdR6*^{c} allele. The *amdR6*^{c} missense mutation occurs in the middle of the gene, and it is suggested that it results in an altered protein which activates gene expression efficiently in the absence of an inducer.

Control of structural gene expression by a positively acting regulatory gene requires the regulatory product to exhibit a number of functional properties, such as the ability to enter and accumulate in the nucleus, bind to specific *cis*-acting elements or interact with other products that bind these sequences, and activate structural gene expression either directly or indirectly. Furthermore, one or more of these activities must respond to the interaction between a regulatory product and a specific environmental stimulus.

The *amdS* gene of *Aspergillus nidulans* is regulated by a number of positively acting regulatory genes which appear to act additively and independently (24). One of these genes is the *amdR* gene (also known as *intA*), which, in addition, also regulates the expression of genes involved in lactam and omega amino acid catabolism: *lamA/B*, specifying a lactam permease and lactamase; *gabA*, specifying a γ-aminobutyric acid (GABA) permease; and *gatA*, specifying an omega amino acid transaminase (2, 3, 26, 33, 45). Cloning and sequence analysis of the 5′ ends of the *amdS*, *gatA*, and *lam* genes have allowed the identification of related upstream regulatory sequences necessary and sufficient for *amdR*-mediated regulation (24, 45; I. B. Richardson, T. G. Littlejohn, and M. E. Katz, unpublished data).

The *amdR* gene mediates induction of the structural genes by omega amino acids such as GABA or β-alanine. Recessive *amdR* mutations are noninducible, while semidominant *amdR*^{c} mutations result in high-level constitutive expression of one or more of the genes but still retain some response to an inducer. It is of considerable interest to investigate the role of the inducer in this system. Cloning and preliminary characterization of the *amdR* gene have shown that it is constitutively transcribed at a very low level. Dosage studies with multicopy transformants have shown that increased levels of the *amdR* product lead to elevated structural gene expression and that DNA binding does not appear to be inducer dependent. However, the inducer is required for maximal activation of gene expression (1). Mobility shift assays using crude nuclear extracts have shown that the *amdR* product binds to specific DNA fragments containing the proposed binding site in the absence of added inducer (R. van Heejswyck and M. J. Hynes, unpublished data).

The sequencing, transcriptional mapping, and analysis of the *amdR* gene and its predicted product are described here. In addition, the mutant lesion in the *amdR6*^{c} constitutive allele was located by the use of a rapid method using *A. nidulans* transformation and found to result from a single missense mutation. The implications of the nature and position of this mutation for the role of the inducer in *amdR*-mediated regulation are discussed.

Many regulatory proteins possess a number of discrete functional domains and show a capacity to tolerate deletions of other regions with little or no effect on their activity. Simple deletion techniques coupled with in vivo assays have been used to analyze numerous regulatory genes, including the *Saccharomyces cerevisiae GAL4* (29), *HAP1* (42), *ADR1* (5), and *GCN4* (22) genes and a number of mammalian steroid hormone receptor protein genes (14). These studies have led to the identification of various functional characteristics of the regulatory proteins, such as DNA-binding motifs and transcription activation domains (43) and nuclear localization sequences (20, 30, 31, 40, 49). A preliminary dissection of the *amdR* gene is described here. A series of deletion clones of *amdR* were generated and analyzed in vivo by transformation of wild-type and *amdR44* mutants of *A. nidulans*.

MATERIALS AND METHODS

Strains. The genotypes of the *A. nidulans* strains used in this work are shown in Table 1 and have been previously

* Corresponding author.

TABLE 1. Details of strains used

Strain	Genotype[a]
MH6	*biA1 amdR6^c niiA4*
MH345	*biA1 amdR44 pyroA4 niiA4*
MH1574	*yA1 acrA1 galA1 pyroA4 hxA1 nicB8 riboB2*
MH3085	*yA1 amdR44 prn-309 riboB2*
Wild type	*biA1 niiA4*
J9	*pabaA1 prn-309 cnxJ1*

[a] The meanings of the gene symbols are given in reference 11.

described (1). Appropriate mutant strains were generated by standard meiotic crosses.

Media and growth conditions. Media and growth conditions were as previously described (23). Nitrogen sources were used at a final concentration of 10 mM, and the carbon source was 1% (wt/vol) D-glucose unless otherwise stated.

Transformation of *A. nidulans*. Preparation of *A. nidulans* protoplasts and transformation were performed as described previously (1). Cotransformation experiments used the pAN222 plasmid (13), containing nearly all of the *A. nidulans prn* gene cluster, as the selected marker. Following transformation into an appropriate *prn-309*-containing strain and selection on medium containing proline as a sole nitrogen source, these *prn*$^+$ transformants were screened on the appropriate media for *amdR*-controlled activities. Transformation of *A. nidulans* protoplasts, using single-stranded or double-stranded M13-based *amdR* clones, was performed with no modifications to the normal transformation procedure.

DNA sequencing. DNA sequencing was performed by the dideoxynucleotide triphosphate chain termination method of Sanger et al. (48) using single-stranded M13 subclones or by generating nested deletions by the method of Dale et al. (12). Nearly all clones for the *amdR*$^+$ and *amdR6*^{c} mutant genes were sequenced at least twice. Sequencing reaction products were fractionated on 4% polyacrylamide–7 M urea field gradient gels as described by Chen and Seeburg (9). The *amdR* sequence information has been lodged with GenBank (accession no. M31517).

S1 nuclease mapping. Mapping of the *amdR* transcription start points, endpoints, and intron boundaries was performed by S1 nuclease mapping. Radiolabeled probes for S1 mapping were produced by the method of Burke (8). The single-stranded ^{32}P-labeled probes were purified from the templates by denaturing in an equal volume of 60% dimethyl sulfoxide in 10 mM Tris hydrochloride (pH 8.0) at 100°C for 3 min, followed by quenching in ice, fractionating on a 1.2% neutral agarose gel, and electroeluting the probe after brief autoradiographic localization and excision of the desired fragment from the gel. *A. nidulans* poly(A)$^+$ RNA was isolated as previously described (25).

Hybridization of the single-stranded radiolabeled probes with 20 μg of poly(A)$^+$ RNA and subsequent digestion with a range of final S1 nuclease concentrations were performed as described by Burke (8). The use of a range of final S1 nuclease concentrations permitted discrimination between S1-dependent and mRNA-dependent heterogeneity in the reaction products. The S1 digestion products were fractionated on either 4 or 6% polyacrylamide–7 M urea field gradient sequencing gels, with concurrently run sequencing reaction ladders used for size determination.

General molecular methods. The general molecular methods used were described previously (1, 25). Southern blotting of DNA was performed with nylon membranes (Zetaprobe; Bio-Rad Laboratories) by the method of Reed and Mann (44). DNA dot blotting for copy number determination was performed by serially diluting (10-fold) approximately equal amounts of genomic *A. nidulans* transformant and control recipient strain DNA. The DNA samples were denatured in 0.4 M NaOH and dotted onto nylon membranes by using a 96-DOTTER filtration manifold (Schleicher & Schuell, Inc.). The blots were initially probed with a gel-purified *amdR*-specific probe and autoradiographed without an intensifying screen, and the probe was washed off. The blots were then reprobed with a gel-purified *amdS*-specific fragment. After densitometric screening of the autoradiographs, the results obtained with the *amdS* probe were used to correct for variations in DNA concentration and the results obtained with the control recipient strain samples were used for *amdR* single-copy number corrections.

Deletion clones. The *amdR* deletion subclones used for the complementation and competition studies were generated from various full-length *amdR*$^+$ clones by using appropriate restriction sites to either delete a specific region from the parent clone or to isolate a specific region for subcloning into pBR322, pUC13, or M13mp19 vectors. All deletion clones were extensively restriction mapped and/or sequenced to confirm their identities.

The subclones of the *amdR6*^{c} mutant gene used to identify the region carrying the mutant lesion were generated by subcloning specific regions from the full-length pALX-16 clone into either M13mp18 or M13mp19 vectors.

RESULTS

Physical structure of *amdR*. The entire nucleotide sequence of a 4.2-kilobase (kb) *Cla*I-*Eco*RI fragment of *amdR*, capable of fully complementing all *amdR* activities, was determined from both strands by the dideoxynucleotide chain termination method. The sequence of the gene and the deduced *amdR* protein sequence of 756 amino acids are presented in Fig. 1.

Open reading frame analysis and comparison of the *amdR* sequence with consensus sequences for filamentous-fungus introns identified three putative introns within the previously defined *amdR* transcribed region, two of which would span an exon of only four nucleotides. S1 nuclease mapping (Table 2) confirmed the presence of the 5′ intron, and the data were entirely consistent with the locations of the remaining two introns predicted by the sequence and open reading frame analysis. The sizes of these three introns were 88, 99, and 57 nucleotides. No other introns were detected within *amdR* by this S1 analysis.

The 5′ transcription initiation region showed significant heterogeneity over two short regions, with three major initiation sites evident. Similarly, the 3′ end of the *amdR* mRNA exhibited heterogeneity, corresponding to two short distinct regions with no major sites. Comparison of the predicted sizes of the *amdR* mRNA from S1 mapping experiments (2,629 to 2,664 nucleotides) and Northern (RNA) blot analysis (2,700 nucleotides) showed good correlation.

Previous Northern analysis of *amdR* had defined a second mRNA of 1.8 kb which showed homology to the *amdR* gene (1). Confirmed homology between this mRNA and *amdR* was confined to a very short region (270 base pairs [bp]) of *amdR* and, through S1 nuclease mapping, the homology was shown not to be perfect. This suggested that the 1.8-kb

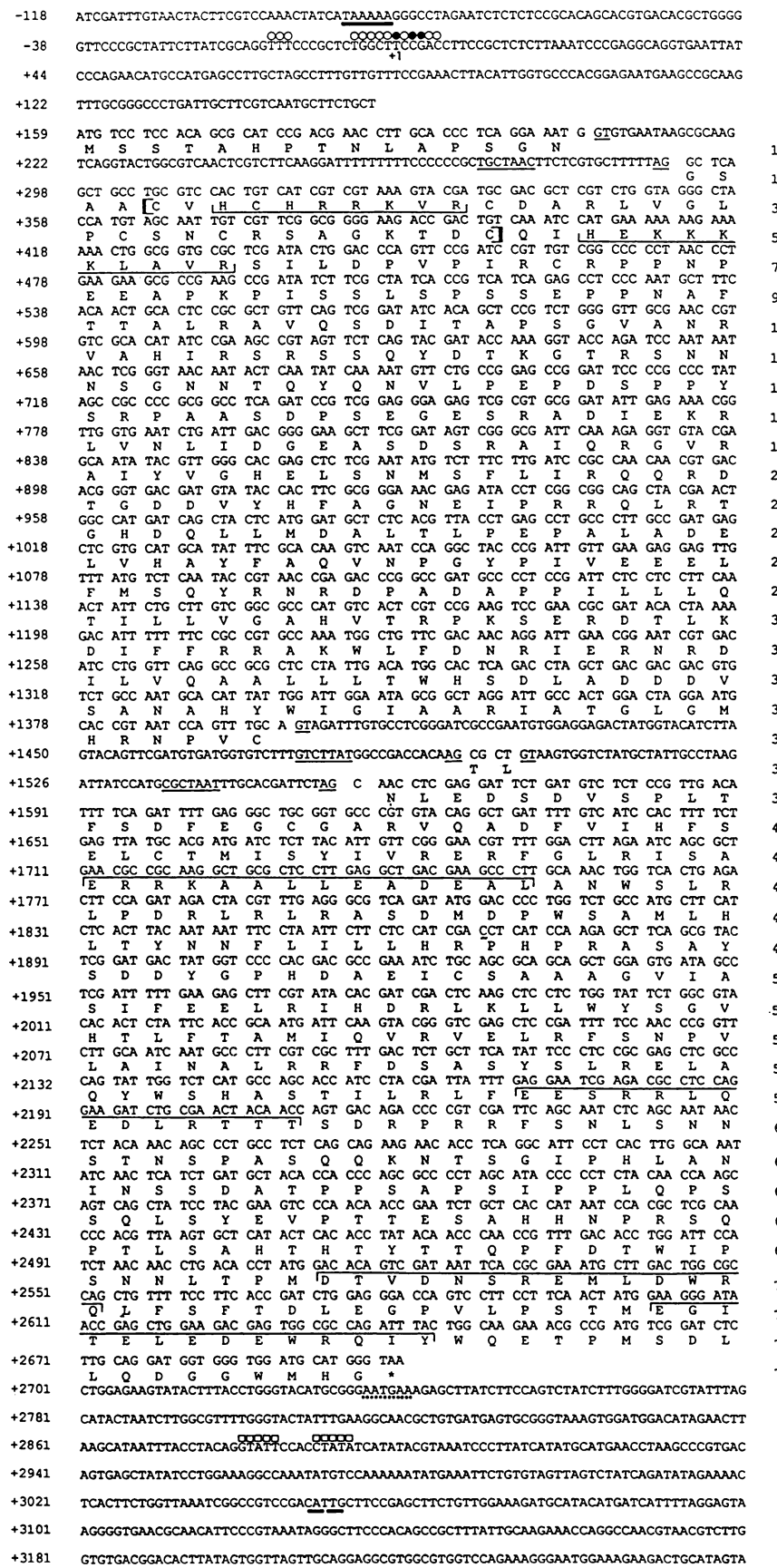

TABLE 2. S1 mapping data

Probe	Location (nucleotides)	Size (bases)	Protected fragment(s) (bases)
MR-5/1	−118 to +296	416	198–208, 216–219[a]
MR-6/2	+296 to +800	504	504–508[b]
MR-10/2	+1015 to +1923	919	378–380, 386–388[c]
ALX-5/4	+1561 to +2313	752	752–756[b]
19/5X/RV-1	+2709 to +3436	727	168–172, 177–181[d]
19/4 ES-6	+3436 to +4179	740	None

[a] Two 5′ transcription initiation regions exhibiting heterogeneity.
[b] S1 concentration-dependent heterogeneity.
[c] Two fragments exhibiting S1 concentration-dependent heterogeneity and believed to represent exon sequences flanking two introns separated by an unusually short 4-bp exon.
[d] Two 3′ mRNA endpoints exhibiting heterogeneity.

mRNA was not *amdR* derived, and subsequent Southern analysis of *A. nidulans* genomic DNA using probes covering this region identified non-*amdR*-derived, weakly hybridizing fragments (data not shown). Hence, it was clear that other sequences within *A. nidulans*, which produced a 1.8-kb transcript, shared limited homology with a short region of *amdR*.

Examination of the 5′ region of *amdR* failed to show any homology to the putative *amdR* upstream regulatory sequence, which is consistent with Northern analysis of *amdR* transcription that showed that the *amdR* 2.7-kb mRNA is constitutively transcribed at low levels and that a functional *amdR* product is not required for its expression (1). General promoter elements within the 5′ region of *amdR* included a TATA-like sequence beginning at −86 and numerous pyrimidine-rich sequences that surround and overlap both the minor and major transcription initiation sites of *amdR*. Pyrimidine-rich sequences surrounding the transcription initiation site have been noted in a number of filamentous fungal genes (19).

Examination of the 3′ region of the *amdR* gene identified a number of sequences which have been previously shown to be involved in transcription termination and 3′ processing (7). These include a number of AT-rich sequences which may play a role in transcription termination, an AAUAAA-homologous sequence at 140 bases upstream of the first mapped mRNA end site, a number of GT-rich regions predominantly upstream of the mRNA end sites which may be involved in 3′ processing, and the CAYTG motif at 155 bases downstream of the 3′-most S1-mapped mRNA end site (Fig. 1).

The 5′ transcribed region of *amdR* contains four AUG codons, not including the AUG initiator of the major open reading frame, beginning at positions +51, +56, +110, and +148. The AUG of the major open reading frame begins at +159 (Fig. 1). These four upstream AUG codons constitute short open reading frames of 2, 26, 8, and 38 amino acids, where the fourth open reading frame actually overlaps the *amdR* coding region. Their significance (if any) is unknown.

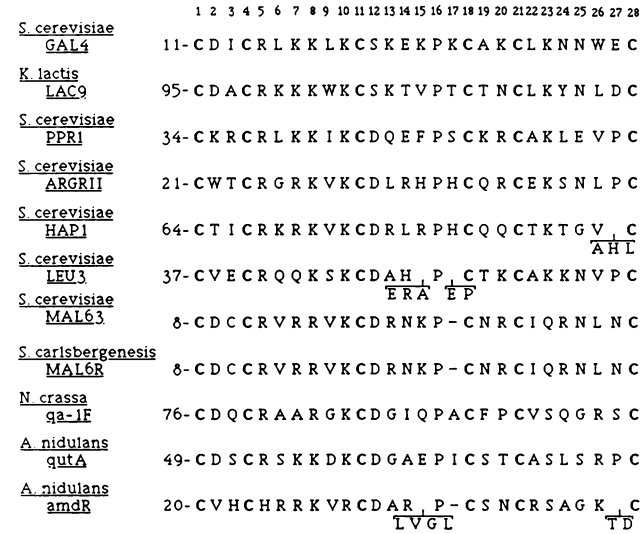

FIG. 2. Comparison of C_6 zinc fingers DNA-binding motifs. (A) Amino acid comparison of the C_6 cysteine-rich DNA-binding motifs from analyzed fungal regulatory gene products. The sequences are arranged for maximum alignment of conserved amino acids, and the numbers at the start of each sequence refer to the amino acid position of the first cysteine residue of this motif in the protein. The cysteine residues of these motifs are highlighted (bold type). The presented amino acid sequences are as follows: *GAL4* (37), *LAC9* (47, 53), *PPR1* (32), *ARGRII* (39), *HAP1* (42), *LEU3* (16), *MAL63* (35), *MAL6R* (50), *qa-1F* (4), *qutA* (6). (B) Consensus sequence derived on the basis of amino acid identity and polarity, where x denotes any amino acid, p denotes polar amino acids, and a denotes apolar amino acids. The frequency of these amino acids is presented below the consensus.

Predicted *amdR* protein. The predicted *amdR* protein sequence exhibits several interesting features with regard to its role as a positively acting regulator. A cysteine-rich region, homologous to the C_6 subgroup of "zinc finger" DNA-binding motifs found in fungal regulatory genes (15), is present near the N-terminal end (Fig. 1). Comparison of this domain with the derived consensus sequence for the C_6 subgroup shows very strong homology (Fig. 2).

The predicted *amdR* protein sequence is relatively acidic (net charge, −12), and a number of regions within the *amdR* protein show clustering of acidic residues, particularly at the C-terminal end where a net charge of −12 occurs between

FIG. 1. Genomic DNA sequence of the *amdR* gene. The derived nucleotide and predicted protein sequences for the *amdR* gene are presented, with the main features highlighted. The 5′ untranslated sequence shows the TATA-like motif (thick underline), major transcription initiation sites (●), and minor transcription initiation sites (○). The 5′-most major transcription initiation site has been assigned the +1 coordinate. The predicted amino acid sequence of the *amdR* protein is indicated below the DNA sequence. Introns are shown as continuous sequences, and the 5′ GT dinucleotide, 3′ AG dinucleotide, and 3′ splice signals are marked (thin underlines). The 3′ untranslated sequence shows the mRNA end sites (□) and sequences believed to be involved in transcription termination, 3′ processing, and polyadenylation, such as the AATAAA-like motif (dotted underline) and a CAYTG motif (broken underline). The site of the C-to-T transition mutation at +1867 for the *amdR6*[c] gene is marked (wavy underline). The highlighted features of the predicted protein sequence are the cysteine-rich DNA-binding motif ([ ]), the nuclear localization motif homologies (|___|), and the four putative transcription activation motifs (⌈¯¯⌉). The nucleotide sequence coordinates (left-hand side) and amino acid sequence coordinates (right-hand side) are presented.

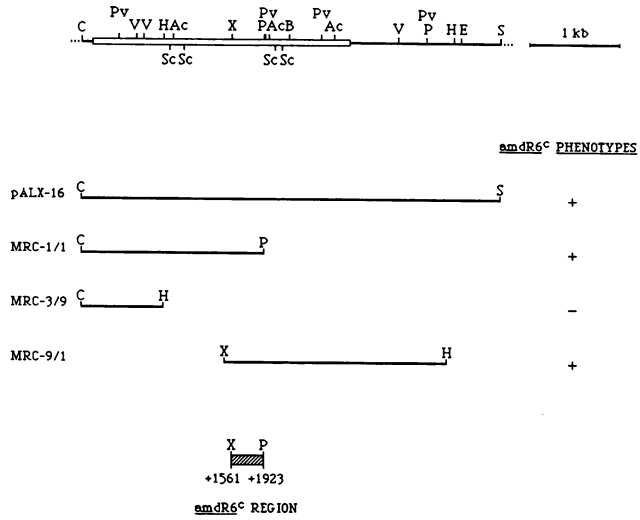

FIG. 3. Localization of the *amdR6*^{c} lesion by transformation. (Top) Map of the *amdR* genomic region showing the relevant restriction sites and the transcribed region (open bar). The *amdR6*^{c} control clone, pALX-16, and the various subclones shown were used to localize the *amdR6*^{c} lesion by transforming these clones into a wild-type *amdR*$^+$ strain and scoring the resultant transformants for an *amdR6*^{c} phenotype. Pluses indicate clones capable of yielding *amdR6*^{c} transformants by recombination with the genomic *amdR*$^+$ gene. On the basis of this analysis, the region of this mutant gene which contains the *amdR6*^{c} mutation corresponds to the *Xho*I-*Pst*I region, denoted by the hatched bar with the flanking restriction sites and sequence coordinates (bottom). The restriction sites indicated are as follows: Ac, *Acc*I; B, *Bgl*II; C, *Cla*I; E, *Eco*RI; H, *Hin*dIII; P, *Pst*I; Pv, *Pvu*II; S, *Sal*I; Sc, *Sac*I; V, *Eco*RV; X, *Xho*I.

amino acids 692 and 759. Calculations of the secondary structure of the *amdR* protein based on the parameters of Chou and Fasman (10) predict the presence of α-helical structures encompassing three of the four acidic regions. Arrangement of these four regions into an α-helical conformation shows that they all exhibit amphipathy, with the acidic residues predominantly aligned along one side of the helix. The three predicted amphipathic α-helices begin at amino acids 437, 589, and 734. The fourth acidic region, which exhibits the strongest amphipathy when arranged into an α-helical conformation, begins at amino acid 704 but was not predicted to form an α-helix.

Two sequences at the amino-terminal end exhibit strong homology to the highly basic nuclear localization motif found in the simian virus 40 large T antigen and other nuclear proteins (30, 31). The first sequence, HCHRRKVR, beginning at amino acid 22, is arginine rich and contains only one lysine residue, while the second sequence, HEKKK KLAVR, beginning at amino acid 53, is very lysine rich and more closely resembles the simian virus 40 large T motif. Only one region within *amdR* shows any homology to the *S. cerevisiae* α2 nuclear localization motif (20), where the pentapeptide core begins at amino acid 456 of *amdR*. However, the *amdR* sequence contains a charged amino acid in this region, while the α2-like sequences contain hydrophobic residues exclusively.

Mapping and sequencing the *amdR6*^{c} mutant gene. The *amdR6*^{c} mutant allele results in high semiconstitutive levels of expression for the activities under *amdR* control (26). The *amdR6*^{c} gene was cloned by a gene rescue technique previously described (1). The method devised to map the *amdR6*^{c} mutation was to transform an *amdR*$^+$ strain of *A. nidulans* with a number of *amdR6*^{c} subclones (Fig. 3). DNA prepared from these M13mp19-based subclones (double stranded and single stranded) was cotransformed into the *amdR*$^+$ *prn-309* strain J9, using pAN222. The *prn*$^+$ transformants were screened for those with an *amdR*^{c} phenotype on medium containing acetamide, acrylamide, or 2-pyrrolidinone as the sole nitrogen source; *amdR*^{c} strains exhibit strong growth on these media compared with *amdR*$^+$ strains.

Of these subclones, only MRC-1/1 and MRC-9/1 yielded *amdR*^{c} transformants, presumably as a result of a double recombination or gene conversion event between the *amdR* region containing the lesion and the resident *amdR*$^+$ gene (Fig. 3). The frequency of transformants obtained with MRC-1/1 and MRC-9/1 by using double-stranded (replicative-form) DNA was not significantly different from that obtained with single-stranded DNA. Considering the regions of *amdR* represented by these subclones, it appeared that the *amdR6*^{c} mutation mapped within a 362-bp *Xho*I-*Pst*I region (Fig. 3). This region was sequenced, and comparison with the wild-type *amdR* sequence of this region showed that the *amdR6*^{c} mutation was the result of a single C-to-T transition at nucleotide position +1867 (Fig. 1). The mutation is predicted to result in a proline-to-serine missense mutation at amino acid 489 of the *amdR* product. The region encompassing this mutation does not coincide with any of the sequence-predicted domains of the *amdR* product.

***amdR* function in *amdR* deletion constructs.** A series of deletion subclones were generated containing either 5′, 3′, or internal deletions of the wild-type *amdR*$^+$ gene (Fig. 4). The deletion clones, vector controls, and wild-type *amdR*$^+$ control clones were individually cotransformed into an *amdR44 prn-309* strain of *A. nidulans* (MH3085), using the *prn*$^+$ plasmid pAN222 as the selectable plasmid. At least 100 proline-utilizing transformants derived from each clone were scored on medium containing GABA, 2-pyrrolidinone, β-alanine, or acetamide as the sole nitrogen source. None of the transformants derived from the vector control plasmids or from pAN222 only exhibited phenotypes different from those of the recipient strain. Transformants from the *amdR*$^+$ control clone exhibited either full wild-type complementation or copy number-dependent elevated levels of structural gene expression above that of the wild type, as previously noted (1).

Of the deletion clones transformed into the loss-of-function *amdR44* mutant, only pALX-40 and pALX-2 showed any transcription activation function (Fig. 4). These deletion subclones lacked sequences 3′ to nucleotide positions +2553 (pALX-40) and +2197 (pALX-2). The predicted proteins derived from these clones are such that pALX-40 possesses amino acids 1 to 718 of *amdR* with 5 extra amino acids derived from readthrough into the pBR322 vector, while pALX-2 possesses amino acids 1 to 598 of *amdR*, with 87 amino acids corresponding to readthrough into pBR322 (Fig. 4).

Transformants derived from these two 3′ deletion clones exhibited only partial complementation of the *amdR44* mutant allele. Growth on medium containing GABA or 2-pyrrolidinone was clearly stronger than the nitrogen-free growth of the recipient strain but not as strong as that of an *amdR*$^+$ strain (Fig. 5). However, growth of these transformants on medium containing acetamide as a sole nitrogen source was stronger than that of the wild type but not as strong as that of an *amdR6*^{c} strain. This effect, as with those on other media, was clearly copy number dependent, as suggested from outcrosses of four representative transfor-

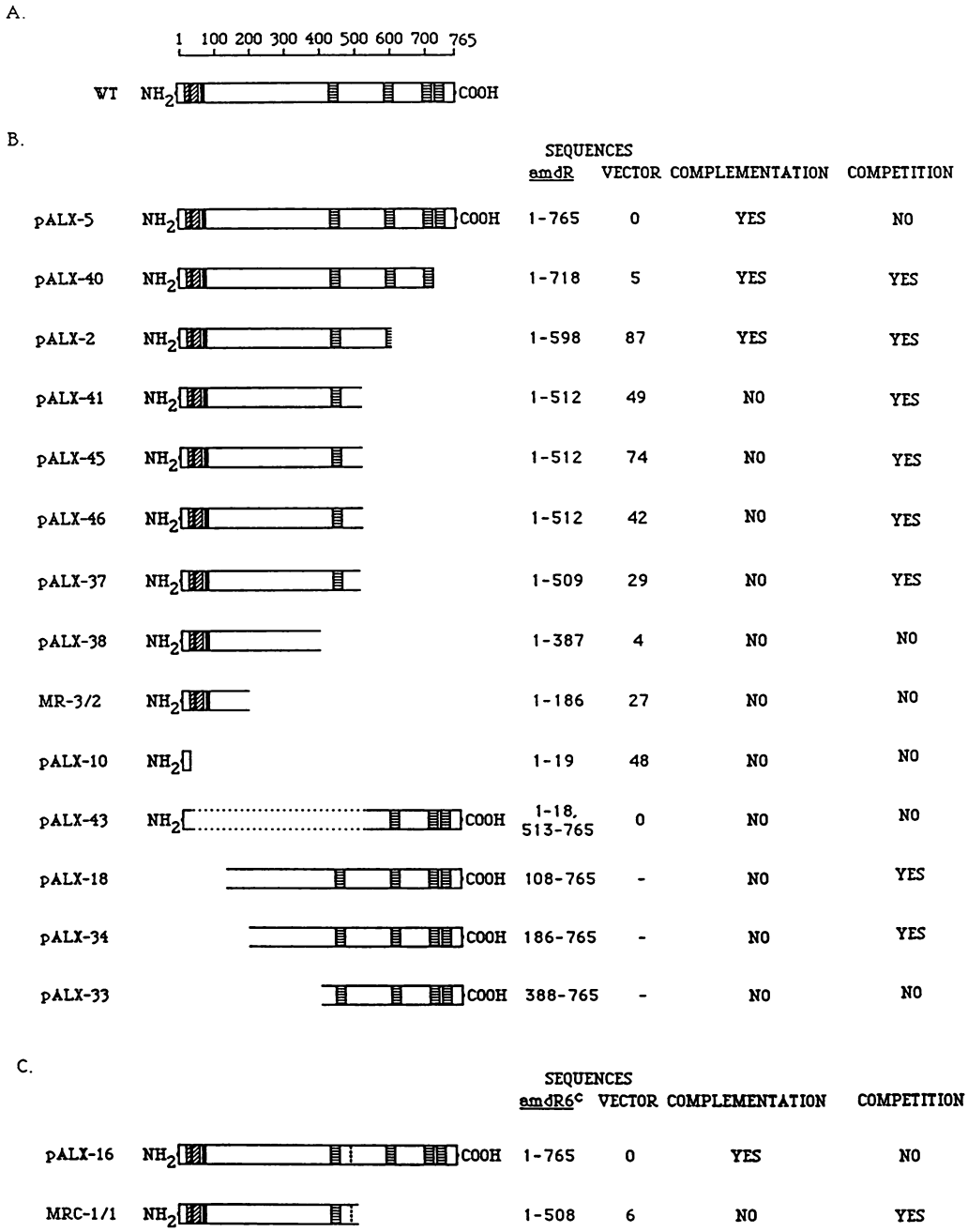

FIG. 4. Complementation and competition analysis of the *amdR*$^+$ and *amdR6*^{c} deletion clones. (A) Diagrammatic representation of the *amdR* product showing the C_6 DNA-binding motif (▨), the putative nuclear localization sequences (■), and the four proposed transcription activation motifs (▤). The scale represents amino acids. (B). Diagrammatic representations of the *amdR*$^+$ control and deletion subclone products. The exact *amdR*-encoded endpoints of each deletion product are indicated, and any vector-encoded additional amino acids in these products derived by readthrough into non-*amdR* sequences before a translation termination codon are also shown. The dotted lines shown for the pALX-43 product represent the deleted internal region of *amdR*, and the dashes under the VECTOR subheading for the pALX-18, -34, and -33 products indicates uncertainty as to the presence of any non-*amdR* sequences in these products (see the text for explanation). Transformation of these deletion clones into an *amdR* mutant of *A. nidulans* and subsequent screening of transformants for complementation of the *amdR* mutant phenotype yielded the results indicated in the COMPLEMENTATION column. Transformation of these deletion clones into an *amdR*$^+$ strain of *A. nidulans* and screening of the transformants for competition phenotypes yielded the results indicated in the COMPETITION column. (C) Diagrammatic representation of the *amdR6*^{c} control and deletion subclone products and the results obtained from the complementation and competition analyses. The position of the *amdR6*^{c} mutation at amino acid 489 is indicated (vertical broken line).

mants from each clone, in which the progeny exhibited a range of phenotypes on the various media similar to the phenotypic variation noted among the primary transformants. Such phenotypic variation among progeny from outcrosses, due to meiotic instability of multiple copies, has been previously noted (34). Determination of *amdR* deletion clone copy numbers in a representative group of transformants by densitometric analysis of genomic DNA dot blots

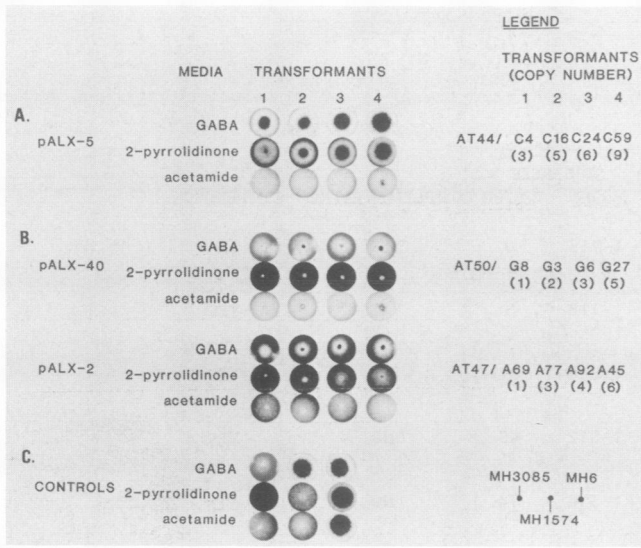

FIG. 5. Representative transformants from the complementation analysis. The growth characteristics of four representative transformants from each of the *amdR*$^+$ complementing clones and relevant control strains are shown on media containing GABA, 2-pyrrolidinone, or acetamide as the sole nitrogen source. The legend indicates the assigned name of each transformant or control strain for reference to the growth characteristics, with the determined copy numbers of each clone in these transformants indicated in parentheses directly below the transformant designation. (A) Transformants from the pALX-5 control clone, which contains the complete *amdR*$^+$ gene. (B) Transformants from the pALX-40 and pALX-2 clones, which contain 3′ deletions of the *amdR*$^+$ gene and produced transformants with partial complementation phenotypes. (C) Growth characteristics of the *amdR44* recipient strain (MH3085), an *amdR*$^+$ strain (MH1574), and an *amdR6*^{c} strain (MH6) used as controls.

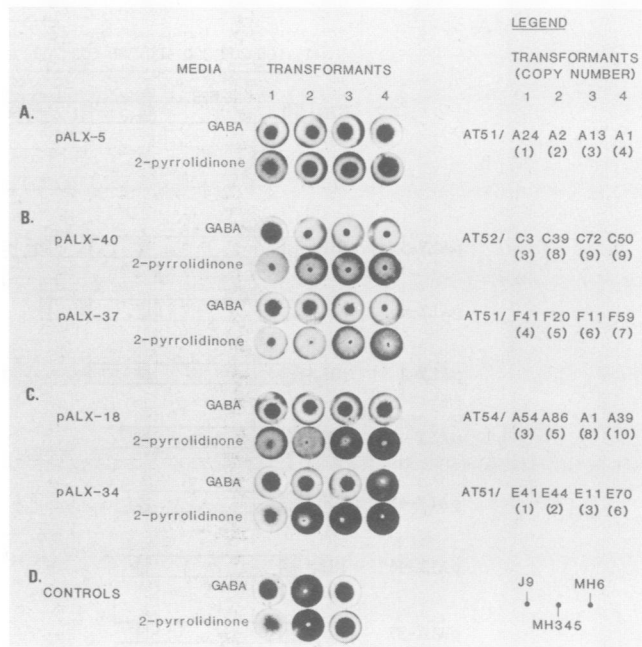

FIG. 6. Representative transformants from the competition analysis. The growth characteristics of four representative transformants from a number of the *amdR*$^+$ competing clones are shown on media containing either GABA or 2-pyrrolidinone as the sole nitrogen source. The legend indicates the assigned name of each transformant or control strain for reference to the growth characteristics, with the determined copy numbers of each clone in these transformants indicated in parentheses directly below the transformant designation. (A) Transformants from the pALX-5 control clone, which contains the complete *amdR*$^+$ gene. (B) Transformants from the 3′ deletion clones carrying the smallest deletion (pALX-40) and the largest deletion (pALX-37), which produced transformants with the competition phenotypes. (C) Transformants from the 5′ deletion clones carrying the smallest deletion (pALX-18) and the largest deletion (pALX-34), which yielded transformants with the competition phenotypes. (D) Growth characteristics of the *amdR*$^+$ recipient strain (J9), an *amdR44* strain (MH345), and an *amdR6*^{c} strain (MH6) used as controls.

showed a clear correlation between copy number and the strength of growth on the various media.

A clear distinction between the effects of the pALX-40- and pALX-2-derived subclones was evident. At a given copy number, pALX-40 transformants showed stronger growth on 2-pyrrolidinone or acetamide than pALX-2 transformants. No difference between these transformants on GABA medium was noted.

Competition by *amdR* deletion products. The *amdR* deletion plasmids were also transformed into the *amdR*$^+$ strain J9 by cotransformation with pAN222. Some of these deletion clones yielded transformants with a partial *amdR* mutant phenotype, as shown by weaker growth on media containing 2-pyrrolidinone or GABA as the sole nitrogen source. No differences between transformants and the recipient strain could be detected on medium containing β-alanine or acetamide as the sole nitrogen source probably because these substrates are already very poor nitrogen sources. None of the transformants derived from the vector control plasmids or from pAN222 alone showed phenotypes different from those of the recipient strains. The partial *amdR* mutant phenotype observed was termed the competition phenotype.

Of the nine 3′ deletion clones transformed into the *amdR*$^+$ strain, six clones representing four different *amdR* deletion endpoints yielded transformants with the competition phenotype (Fig. 4). These six clones represent *amdR* deletion endpoints at +2553 (pALX-40), +2197 (pALX-2), +1936 (pALX-41, -45, -46), and +1929 (pALX-37). The predicted proteins derived from these deletion clones contain amino acids 1 to 718 (pALX-40), 1 to 598 (pALX-2), 1 to 512 (pALX-41, -45, -46), and 1 to 509 (pALX-37), with various stretches of non-*amdR* readthrough sequences.

Comparisons of transformant phenotypes on GABA or 2-pyrrolidinone medium with copy number estimates derived by densitometry of genomic DNA dot blots showed that competition was clearly copy number correlated. Low-copy-number transformants showed competition only on 2-pyrrolidinone, and higher copy numbers extended the effect to GABA (Fig. 6). However, similar copy number transformants derived from different deletion clones did not appear equally proficient in effecting the competition phenotype. It was clear that, at least in some cases, the severity of the competition phenotype was affected by the readthrough sequences. The pALX-41, -45, and -46 clones all bear *amdR* deletion endpoints at +1937 but have different readthrough sequences, and transformants obtained with these clones exhibited different strengths of competition at a given copy number. Examination of these non-*amdR* amino acid sequences for the deletion clones failed to show any distinct trends in charge, hydropathy, or general amino acid composition.

Of the three 5′ deletion clones transformed into the *amdR*$^+$ strain, two yielded transformants with competition phenotypes (Fig. 4). These two clones represented 5′ dele-

tion of *amdR* at +568 (pALX-18) and +800 (pALX-34). The competition phenotypes exhibited by these transformants were identical to those of the 3′ deletion clone transformants. A clear distinction between the degree of competition exhibited by transformants at a given copy number of PALX-18 or pALX-34 was evident (Fig. 6). As described above, readthrough sequence effects may also be operating in any vector sequences present in these products.

These 5′ deletion constructs lack the *amdR* transcription and translation initiation signals, and so to be expressed in *A. nidulans* expression must be driven from cryptic promoter elements present in the vector sequences of these clones; therefore, the exact amino-terminal ends of these products were unknown. As a result, it was not possible to draw any conclusions regarding the lack of competition exhibited by pALX-33 (Fig. 4).

In vivo analysis of an *amdR6*^{c} deletion clone. A 3′ deletion of the *amdR6*^{c} mutant gene was used to test for any partial complementation or competition effects. This deletion clone (MRC-1/1), deleted at nucleotide position +1928 and so still possessing the *amdR6*^{c} mutation, was equivalent to the pALX-37 deletion clone of the *amdR*$^+$ gene (Fig. 4). Cotransformation of MRC-1/1 into a loss-of-function *amdR44* mutant of *A. nidulans* did not yield any transformants showing any degree of complementation, as was also noted for pALX-37. Cotransformation of this *amdR6*^{c} deletion clone into an *amdR*$^+$ strain (J9) of *A. nidulans* yielded transformants with the competition phenotype. These transformants also showed a clear correlation between plasmid copy number and the degree of competition, and the observed phenotypes were similar to those of the *amdR*$^+$ deletion transformants. However, transformants from the *amdR*$^+$ pALX-37 deletion clone showed stronger competition than MRC-1/1-derived transformants at a given copy number (data not shown).

DISCUSSION

Previous genetic analysis has shown that the *amdR* gene controls the expression of five structural genes involved in the utilization of various substrates as carbon and/or nitrogen sources in response to omega amino acid inducers. Cloning and analysis of the *amdR* gene have shown that it is constitutively transcribed at a very low level and that this low-level expression, coupled with limiting concentrations of inducer under noninducing conditions, appears to be the governing determinant of basal level structural gene expression. Similarly, the level of the *amdR* product, determined by its constitutive expression, appears also to set the upper level of structural gene expression under inducing conditions (1). The results presented here describe the physical structure of the *amdR* gene and provide an initial characterization of *amdR* function.

The predicted *amdR* amino acid sequence contains two small regions homologous to a motif identified in the simian virus 40 large T antigen and shown to be sufficient and necessary for nuclear localization (30, 31). Similar results have been obtained with homologous sequences in the *Xenopus laevis* N1 protein and polyomavirus large T antigen. In both of the latter cases two closely spaced homologous sequences are present (36, 46), as is also the case for the *amdR* product. Interestingly, deletion of the N-terminal region containing these two putative nuclear localization sequences in *amdR* did not affect the capacity of the resultant products to compete with the *amdR*$^+$ product in vivo (see below).

The cysteine-rich sequence identified at the amino-terminal end of the predicted *amdR* protein sequence is homologous to the C_6 subgroup of DNA-binding domains found in fungal regulatory products (15). These C_6 motifs have been shown to be essential for the DNA-binding activity of a number of regulatory proteins, and DNA binding appears to be Zn^{2+} dependent (27). Comparison of the *amdR* protein sequence with the derived consensus sequence for this subgroup (Fig. 2) shows a conservative arginine-to-histidine difference at position 5 and a conservative arginine-to-lysine difference at position 10. Other differences between the *amdR* protein motif and most of the other identified C_6 motifs are (i) extra amino acids between the cysteine at position 11 and the proline at position 16, as has also been noted for the *S. cerevisiae LEU3* product; (ii) no amino acids between the proline at position 16 and the cysteine at position 18, as for the *Saccharomyces carlsbergenesis MAL6R* and *S. cerevisiae MAL63* protein motifs; and (iii) an extra amino acid between the cysteines at positions 21 and 28, as for the *S. cerevisiae HAP1* protein motif. These differences between the various motifs are presumably important in order to accommodate differences among the DNA-binding sites. Such an arrangement of the DNA-binding domain in the *amdR* protein means that both of the putative nuclear localization motifs overlap the DNA-binding domain. The significant of such an arrangement remains obscure at this stage in the absence of nuclear localization studies coupled with site-directed mutagenesis of the *amdR* region. Functionally overlapping domains have been noted in other regulatory genes, including *GAL4* (28, 38) and a number of steroid hormone receptor genes (21, 52).

Four regions within the predicted *amdR* protein sequence exhibit clustering of acidic residues such that they exhibit amphipathy when arranged in an α-helical conformation. Similar acidic amphipathic α-helical structures have been shown to possess transcription activation function (18, 43). Complementation analysis of a number of *amdR* deletion clones showed that amino acids 719 to 765 are essential for full activator function of the *amdR* product. The predicted amphipathic α-helix starting at amino acid 734 is contained within this region of the protein. The larger 3′ deletion product from amino acids 599 to 765 showed weaker transcription activator function than that of the product with the shorter deletion, suggesting that the third putative acidic activation domain starting at amino acid 704 may also be functional, despite its predicted lack of α-helical conformation. While these conclusions must remain tentative in light of any possible stability differences or effects due to non-*amdR* readthrough sequences, the results suggest that these deletions do not remove sequences absolutely essential for *amdR* function.

The smallest carboxyl-terminal deletion of *amdR* failing to show any transcription activator function was deleted for amino acids 513 to 765, and this deletion was represented by three clones with different non-*amdR* readthrough sequences. This deletion removed another putative amphipathic α-helix starting at amino acid 590, leaving only the one putative activation sequence, starting at amino acid 437. This indicates that the region from amino acids 513 to 598 may contain sequences essential for structural gene activation in the absence of any carboxyl-terminal *amdR* sequences. Whether this region is also essential for gene activation in the presence of the remaining carboxyl-terminal region of *amdR* cannot be assessed. Therefore, based on this transcription activation analysis, it appears that the *amdR* product contains at least two activation regions in its car-

boxyl-terminal half, each of which may function independently but where both are required for wild-type levels of transcription activation. Other regulatory gene products, including GAL4, ADR1, and hGR, also possess multiple activation domains which are all required for full wild-type activation levels but also appear to function individually (5, 17, 21, 38).

Multiple copies of a number of *amdR* deletion derivatives were observed to result in a partial *amdR* mutant phenotype. Presumably this resulted from the products of these deleted genes interfering with the wild-type product function or competing for a limiting component essential for gene activation. The most obvious way in which this could occur is by competition for DNA-binding sites. However, if it is assumed that the C_6 zinc finger at the amino-terminal end of the *amdR* protein is essential and also sufficient for DNA binding, then it might have been expected that deletion products containing amino acids 1 to 387 (pALX-38) and 1 to 186 (MR-3/2) would have shown competition. This was not observed. Furthermore, two clones with deletions of the 5′ region encoding the C_6 sequence showed competition. Therefore, it is unlikely that competition for DNA-binding sites can explain the results unless the C_6 region is not essential for DNA binding.

If it is assumed that in the 5′ deletion plasmids transcription and translation are occurring so that a partial *amdR* polypeptide is formed, then the common region apparently involved in competition lies between amino acids 186 and 509. This region lacks the putative nuclear localization signals, indicating that competition may not be for nuclear uptake. Subunit mixing represents another possibility by which competition may be effected. Heteromers formed between $amdR^+$ and *amdR* deletion products may result in reduced activation of structural genes, with the region defined by competition analysis containing an essential multimerization domain. However the proposed DNA-binding site for *amdR* lacks dyad symmetry (24, 45), a common feature of sites binding multimeric regulatory proteins.

Competition could be at the level of inducer binding. This would require that effective inducer concentrations be low, given the copy numbers of the various deletion subclones in transformants. In the *amdR* regulon, maintenance of such low inducer concentrations may be essential because of the toxicity associated with high endogenous levels of the inducer GABA (2). For the *S. cerevisiae* galactose-melibiose regulon, it has been suggested that even under galactose-inducing conditions there is insufficient inducer to saturate the *GAL80* protein (41, 51, 54). This hypothesis, however, is difficult to reconcile with recent results which indicate that the same set of deletion clones cause a similar pattern of competition with the $amdR104^c$ mutation (S. A. Mathews, unpublished data). This mutation, like other $amdR^c$ alleles, causes high levels of structural gene expression in the absence of exogenous inducer. Therefore, at present, the mechanism for the competition effects is unclear.

It has been previously suggested that the role of the inducer is to cause an alteration in the conformation of the *amdR* product, greatly increasing its ability to activate transcription (1). In vitro binding assays have shown that an inducer is not necessary for the *amdR* protein to bind to DNA (R. van Heejswyck and M. J. Hynes, unpublished data). The $amdR6^c$ mutation results in a serine-to-proline change at amino acid 489, which would be expected to result in a marked conformational change. It is proposed that this altered protein can efficiently activate gene expression in the absence of added inducer. Addition of inducer results in even stronger activation, and the semiconstitutive $amdR6^c$ phenotype results.

Sequence analysis and preliminary functional dissection of the *amdR* product has suggested the presence of a number of functional domains within the protein. Further analysis of both in vivo- and in vitro-generated mutations will allow a more precise definition of these functions.

ACKNOWLEDGMENTS

This work was supported by the Australian Research Council and a Commonwealth Postgraduate Award to A.A.

Invaluable comments by Imogen Richardson and Meryl Davis are appreciated.

LITERATURE CITED

1. **Andrianopoulos, A., and M. J. Hynes.** 1988. Cloning and analysis of the positively acting regulatory gene *amdR* from *Aspergillus nidulans*. Mol. Cell. Biol. **8**:3532–3541.
2. **Arst, H. N.** 1976. Integrator gene in *Aspergillus nidulans*. Nature (London) **262**:231–234.
3. **Arst, H. N., H. A. Penfold, and C. R. Bailey.** 1978. Lactam utilization in *Aspergillus nidulans*: evidence for a fourth gene under the control of the integrator gene *intA*. Mol. Gen. Genet. **166**:321–327.
4. **Baum, J. A., R. Greever, and N. H. Giles.** 1987. Expression of *qa-1F* activator protein: identification of upstream binding sites in the *qa* gene cluster and localization of the DNA-binding domain. Mol. Cell. Biol. **7**:1256–1266.
5. **Bemis, L. T., and C. L. Denis.** 1988. Identification of functional regions in the yeast transcriptional activator *ADR1*. Mol. Cell. Biol. **8**:2125–2131.
6. **Beri, R. K., H. Whittington, C. F. Roberts, and A. R. Hawkins.** 1987. Isolation and characterization of the positively-acting regulatory gene *gutA* from *Aspergillus nidulans*. Nucleic Acids Res. **15**:7991–8001.
7. **Birnstiel, M. L., M. Busslinger, and K. Strub.** 1985. Transcription termination and 3′ processing: the end is in site! Cell **411**:349–359.
8. **Burke, J. F.** 1984. High-sensitivity S1 mapping with single-stranded [^{32}P] DNA probes synthesized from bacteriophage m13mp templates. Gene **30**:63–68.
9. **Chen, E. Y., and P. H. Seeburg.** 1985. Supercoil sequencing: a fast and simple method for sequencing plasmid DNA. DNA **4**:165–170.
10. **Chou, P. Y., and G. D. Fasman.** 1978. Empirical predictions of protein conformation. Annu. Rev. Biochem. **47**:251–276.
11. **Clutterbuck, A. J.** 1984. Loci and linkage map of the filamentous fungus *Aspergillus nidulans*, p. 265–273. *In* S. J. O'Brien (ed.), Genetic maps, vol. 3. Cold Spring Harbor Laboratory, Cold Spring Harbor, N.Y.
12. **Dale, R. M. K., B. A. McClure, and J. P. Houchins.** 1985. A rapid single-stranded cloning strategy for producing a sequential series of overlapping clones for use in DNA sequencing. Application to sequencing the corn mitochondrial 185 rDNA. Plasmid **13**:141–151.
13. **Durrens, P., P. M. Green, H. N. Arst, and C. Scazzocchio.** 1986. Heterologous insertion of transforming DNA and generation of new deletions associated with transformation in *Aspergillus nidulans*. Mol. Gen. Genet. **203**:544–549.
14. **Evans, R. M.** 1988. The steroid and thyroid hormone receptor superfamily. Science **240**:889–895.
15. **Evans, R. M., and S. M. Hollenberg.** 1988. Zinc fingers: gilt by association. Cell **52**:1–3.
16. **Friden, P., and P. Schimmel,** 1987. *LEU3* of *Saccharomyces cerevisiae* encodes a factor for control of RNA levels of a group of leucine-specific genes. Mol. Cell. Biol. **7**:2708–2717.
17. **Giguere, V., S. M. Hollenberg, M. G. Rosenfeld, and R. M. Evans.** 1986. Functional domains of the human glucocorticoid receptor. Cell **46**:645–652.
18. **Giniger, E., and M. Ptashne.** 1987. Transcription in yeast activated by a putative amphipathic α-helix linked to a DNA

binding unit. Nature (London) **330**:670–672.
19. **Gurr, S. J., S. E. Unkles, and J. R. Kinghorn.** 1988. The structure and organization of nuclear genes of filamentous fungi, p. 93–139. *In* J. R. Kinghorn (ed.), Gene structure in eukaryotic microbes. IRL Press, Oxford.
20. **Hall, M. N., L. Hereford, and I. Herskowitz.** 1984. Targeting of *E. coli* 2-galactosidase to the nucleus in yeast. Cell **36**:1057–1065.
21. **Hollenberg, S. M., V. Giguere, P. Segul, and R. M. Evans.** 1987. Colocalization of DNA-binding and transcriptional activation functions in the human glucocorticoid receptor. Cell **49**:39–46.
22. **Hope, I. A., and K. Struhl.** 1986. Functional dissection of a eukaryotic transcriptional activator protein, *GCN4* of yeast. Cell **46**:885–894.
23. **Hynes, M. J.** 1972. Mutants with altered glucose repression of amidase enzymes in *Aspergillus nidulans*. J. Bacteriol. **111**: 717–722.
24. **Hynes, M. J., C. M. Corrick, J. M. Kelly, and T. G. Littlejohn.** 1988. Identification of the sites of action of regulatory genes controlling the *amdS* gene of *Aspergillus nidulans*. Mol. Cell. Biol. **8**:2589–2596.
25. **Hynes, M. J., C. M. Corrick, and J. A. King.** 1983. Isolation of genomic clones containing the *amdS* gene of *Aspergillus nidulans* and their use in the analysis of structural and regulatory mutations. Mol. Cell. Biol. **3**:1430–1439.
26. **Hynes, M. J., and J. A. Pateman.** 1970. The genetic analysis of regulation of amidase synthesis in *Aspergillus nidulans*. I. Mutants able to utilize acrylamide. Mol. Gen. Genet. **108**: 97–106.
27. **Johnston, M.** 1987. Genetic evidence that zinc is an essential co-factor in the DNA binding domain of *GAL4* protein. Nature (London) **328**:353–355.
28. **Johnston, S. A., J. M. Salmeron, and S. S. Dincher.** 1987. Interaction of positive and negative regulatory proteins in the galactose regulon of yeast. Cell **50**:143–146.
29. **Johnston, S. A., M. J. Zavortink, C. Debouck, and J. E. Hopper.** 1986. Functional domains of the yeast regulatory protein *GAL4*. Proc. Natl. Acad. Sci. USA **83**:6553–6557.
30. **Kalderon, D., W. D. Richardson, A. F. Markham, and A. E. Smith.** 1984. Sequence requirements for nuclear localization of simian virus 40 large-T antigen. Nature (London) **311**:33–38.
31. **Kalderon, D., B. L. Roberts, W. D. Richardson, and A. E. Smith.** 1984. A short amino acid sequence able to specify nuclear location. Cell **39**:499–509.
32. **Kammerer, B., A. Guyonvarch, and J. C. Hubert.** 1984. Yeast regulatory gene PPRI. I. Nucleotide sequence, restriction map and codon usage. J. Mol. Biol. **180**:239–250.
33. **Katz, M. E., and M. J. Hynes.** 1989. Characterization of the *amdR* controlled *lamA* and *lamB* genes of *Aspergillus nidulans*. Genetics **122**:331–339.
34. **Kelly, J. M., and M. J. Hynes.** 1987. Multiple copies of the *amdS* gene of *Aspergillus nidulans* cause titration of *trans*-acting regulatory proteins. Curr. Genet. **12**:21–31.
35. **Kim, J., and C. A. Michaels.** 1988. The *MAL63* gene of *Saccharomyces cerevisiae* encodes a cysteine-zinc finger protein. Curr. Genet. **14**:319–323.
36. **Kleinschmidt, J. A., and A. Seiter.** 1988. Identification of domains involved in nuclear uptake and histone binding of protein NI of *Xenopus laevis*. EMBO J. **7**:1605–1614.
37. **Laughon, A., and R. F. Gesteland.** 1984. Primary structure of the *Saccharomyces cerevisiae GAL4* gene. Mol. Cell. Biol. **4**: 260–267.
38. **Ma, J., and M. Ptashne.** 1987. Deletion analysis of *GAL4* defines two transcriptional activation segments. Cell **48**:847–853.
39. **Messenguy, F., E. Dubois, and F. Descamps.** 1986. Nucleotide sequence of the *ARGRII* regulatory gene and amino acid sequence homologies between *ARGRII*, *PPRI* and *GAL4* regulatory proteins. Eur. J. Biochem. **157**:77–81.
40. **Moreland, R. B., G. L. Langevin, R. H. Singer, R. L. Garcea, and L. M. Hereford.** 1987. Amino acid sequences that determine the nuclear localization of yeast histone 2B. Mol. Cell. Biol. **7**:4048–4057.
41. **Nogi, Y., H. Shimada, Y. Matsuzaki, H. Hashimoto, and T. Fukasawa.** 1984. Regulation of expression of the galactose gene cluster in *Saccharomyces cerevisiae*. II. The isolation and dosage effect of the regulatory gene *GAL80*. Mol. Gen. Genet. **195**:29–34.
42. **Pfeifer, K., K.-S. Kim, S. Kogan, and L. Guarente.** 1989. Functional dissection and sequence of yeast *HAPI* activator. Cell **56**:291–301.
43. **Ptashne, M.** 1988. How eukaryotic transcriptional activators work. Nature (London) **335**:683–689.
44. **Reed, K. C., and D. A. Mann.** 1985. Rapid transfer of DNA from agarose gels to nylon membranes. Nucleic Acids Res. **13**: 7207–7221.
45. **Richardson, I. B., S. K. Hurley, and M. J. Hynes.** 1989. Cloning and molecular characterization of the *amdR* controlled *gatA* gene of *Aspergillus nidulans*. Mol. Gen. Genet. **217**:118–125.
46. **Richardson, W. D., B. L. Roberts, and A. E. Smith.** 1986. Nuclear location signals in polyoma virus large-T. Cell **44**: 77–85.
47. **Salmeron, J. M., and S. A. Johnston.** 1986. Analysis of the *Kluveromyces lactis* positive regulatory gene *LAC9* reveals functional homology to, but sequence divergence from, the *Saccharomyces cerevisiae GAL4* gene. Nucleic Acids Res. **14**:7767–7781.
48. **Sanger, F., A. R. Coulson, B. G. Barrell, A. J. H. Smith, and B. A. Roe.** 1980. Cloning of single-stranded bacteriophage as an aid to rapid DNA sequencing. J. Mol. Biol. **143**:161–178.
49. **Silver, P. A., A. Chiang, and I. Sadler.** 1988. Mutations that alter both localization and production of a yeast nuclear protein. Genes Dev. **2**:707–717.
50. **Sollitti, P., and J. Marmur.** 1988. Primary structure of the regulatory gene from the *MAL6* locus of *Saccharomyces carlsbergenesis*. Mol. Gen. Genet. **213**:56–62.
51. **Torchia, T. E., C. W. Hamilton, C. L. Cano, and J. E. Hopper.** 1984. Disruption of regulatory gene *GAL80* in *Saccharomyces cerevisiae*: effects on carbon-controlled regulation of the galactose/melibiose pathway genes. Mol. Cell. Biol. **4**:1521–1527.
52. **Webster, N. J. G., S. Green, J. R. Jin, and P. Chambon.** 1988. The hormone-binding domain of the estrogen and glucocorticoid receptors contain an inducible transcription activation function. Cell **54**:199–207.
53. **Wray, L. V., M. M. Witte, R. C. Dickson, and M. I. Riley.** 1987. Characterization of a positive regulatory gene, *LAC9*, that controls induction of the lactose-galactose regulon of *Kluveromyces lactis*: structural and functional relationships to *GAL4* of *Saccharomyces cerevisiae*. Mol. Cell. Biol. **7**:1111–1121.
54. **Yocum, R. R., and M. Johnston.** 1984. Molecular cloning of the *GAL80* gene from *Saccharomyces cerevisiae* and characterization of a *gal80* deletion. Gene **32**:75–82.